ORIGINAL ARTICLE

WILEY Microcirculation

Pericyte modulation by a functional antibody obtained by a novel single-cell selection strategy

Jesper Just[1,2] | Simon Lykkemark[2,3] | Charlotte H. Nielsen[1] | Ali R. Roshenas[4] | Kim R. Drasbek[2] | Steen V. Petersen[5] | Toke Bek[2] | Peter Kristensen[4] (ID)

[1]Department of Molecular Biology and Genetics, Aarhus University, Aarhus C, Denmark

[2]Department of Clinical Medicine, Aarhus University, Aarhus C, Denmark

[3]Sino-Danish Centre for Education and Research (SDC), Aarhus C, Denmark

[4]Department of Engineering, Aarhus University, Aarhus C, Denmark

[5]Department of Biomedicine, Aarhus University, Aarhus C, Denmark

Correspondence
Peter Kristensen, Department of Engineering, Aarhus University, Aarhus C, Denmark.
Email: pk@eng.au.dk

Abstract

Objective: Pericytes surround the endothelial cells of the microvasculature where they serve as active participants in crucial vascular functions such as angiogenesis, stability, and permeability. However, pericyte loss or dysfunction has been described in a number of pathologies. Targeting pericytes could therefore prove instrumental in the further development of vascular therapeutics.

Methods: To target the pericyte, a proteomic-based approach using antibody phage display was conducted. We present a novel single-cell selection strategy, with a modified selection step to drive the selection of antibodies toward relevant pericyte epitopes.

Results: Characterization of the selected antibodies revealed two antibodies with binding specificity for pericytes. The cognate antigen of one of the antibodies was identified as pericyte-expressed fibronectin. This antibody was shown to be a potent inhibitor of pericyte migration and to induce a pro-angiogenic response when included in a pericyte-endothelial cell co-culture angiogenesis assay.

Conclusions: The selection method provides an efficient platform for the selection of functional antibodies which target pericytes. We obtain an antibody that interacts with a fibronectin epitope important for pericyte mobility and functionality. Targeting of this epitope in pathologies where pericytes are implicated could potentially be of therapeutic benefit.

KEYWORDS
angiogenesis, fibronectin, pericyte, phage display, recombinant antibodies

1 | INTRODUCTION

Charles-Marie Benjamin Rouget first described pericytes (PCs) in 1873 as a population of cells surrounding the microvessels. PCs are primarily found around the microvessels where they connect to endothelial cells (ECs) via processes that extend through the basement membrane (BM) and as such belong to the vascular wall.[1,2] The retina and the brain have the highest ratio of PCs to ECs (1:1–1:3),[3] which highlights the special importance of the PC here to ensure central nervous system (CNS) homeostasis.[4–6]

PCs show an elongated stellate-shaped morphology, with an elaborate system of cytoplasmatic branches arising from the cell body that partially ensheathe the endothelium. Through interruptions in the BM, the PC forms direct connections to the EC in a peg-and-socket manner. These connections contain adherence and gap junctions for stability and communication.[7–10]

The PC is a multifunctional cell type serving as a coordinator and effector of vascular functions including angiogenesis, vascular stability,

---

Abbreviations: PC, Pericyte; BM, Basement membrane; EC, Endothelial cells; CNS, Central Nervous System; BBB, Blood–brain barrier; PDGFB, Platelet-derived growth factor subunit B; TGF-beta, Transforming growth factor beta; HBVP, Human Brain Vascular Pericyte; VSMC, Vascular Smooth Muscle Cells; HBMEC, Human Brian Microvascular Endothelial Cells; FN, Fibronectin; MBVP, Mouse Brain Vascular Pericyte; Fab, Fragment antigen-binding; scFv, Single-chain fragment variable; sdAb, Single-domain antibody; HRP, Horseradish peroxidase.

JJ, SL, CHN contributed equally to the work

and blood–brain barrier (BBB) formation.[9,11-15] However, PC dysfunction, or loss, has been described in different pathologies, for example, cancer and neurodegenerative diseases, including diabetic retinopathy.[12,16-19] Within cancer, an overall tendency seems to be increased PC coverage of the vasculature in well-differentiated tumors with low metastatic potential and high growth rate. On the contrary, decreased PC coverage correlates with compromised vascular structure and an increased rate of metastasis.[17,19] Hence, a subtle balance of PC coverage seems to be pivotal for homeostasis of the vasculature. This makes the PC a highly interesting target for drug intervention, supported by the fact that several compounds targeting the PC are currently undergoing clinical trials.[17]

Antibodies have proven to be excellent therapeutic agents due to their ability to bind specific targets with high affinity. Therapeutic antibodies were initially murine derived limiting the therapeutic potential. However, protein engineering has innovated the area and enhanced clinical efficacy. Human antibodies can now be obtained by recombinant antibody technology, and especially, the phage display technique has proven to be a versatile and powerful technology for finding specific antibodies for known antigens (by selection on purified protein). In addition, the technology can be used for discovery of novel biomarkers and clinically relevant antibodies.[20-22] Therefore, selection and isolation of functional human antibodies targeting the PC could represent a significant step forward in obtaining novel vascular therapeutics. When targeting the PCs or ECs in the CNS with therapeutic antibodies, the blood–brain barrier often constitutes an obstacle, which has to be crossed. Bispecific antibodies has been engineered, which on one arm bind the transferrin receptor, mediating transcytosis through the blood brain barrier, and on the other arm targets antigens in the brain.[23]

In the present study, we describe a novel single-cell selection methodology, based on the antibody phage display technology. Phage display relies on the physical genotype–phenotype linkage provided by a filamentous bacteriophage.[24] Display of foreign proteins is achieved by introducing a library of genes into the phage genome in-frame with one of the five coat proteins.[25-28] The produced phage particles will each carry a gene variant from the library inside the phage particle, while the encoded foreign protein is displayed on its surface. For display of antibody fragments (Fab, scFv and sdAb), the minor coat protein pIII is the most attractive display fusion due to its tolerance for display of larger proteins.[29] Isolation of functional antibodies through conventional phage display selections (biopanning on thousands to millions of targets cells) is a challenging and laborious task due to a typically high phage output number that requires screening for identification of functional binders. Moreover, phage antibodies binding highly expressed antigens will dominate the output from conventional selections, whereas antibodies recognizing low-abundance antigens will be less frequent. The bias for high abundant antigens is further enhanced when successive selection and amplification steps are performed. To ensure a high diversity of binders, one strategy is to perform only one round of selection and apply a trypsin sensitive helper phage to increase the proportion of clones selected through antibody–antigen interactions.[30] Other strategies for directing the antibody selection toward isolation of cell type-specific antibodies involve masking of unwanted epitopes prior to the selections[31] or stringent negative selections combined with positive panning on the cell type of interest.[32,33] Negative selection (also called subtraction or depletion) is typically performed on cell types related to the positive cell line to deplete the library for binders recognizing commonly expressed antigens. A method combining single-round selection with extensive subtraction of unwanted library variants has previously been described for isolation of antibodies against single cells in a heterogeneous population.[34,35] The selection strategy presented in this work follows the same principles with exception of the method used to recover phage antibodies bound to the target cell.

For the antibody selections, only a few target cells, PCs, were spiked into a background of millions of irrelevant cells of different cell types. Due to excess of background cells, antibodies binding commonly expressed antigens/epitopes will become adsorbed by these. Antibodies bound to the target cells were recovered by aspiration of individual target cells from the selection slide into a micropipette (Figure 1 and Movie S1). With this method, the selection output was drastically reduced and the ratio of interesting binders increased compared to conventional phage selection methods.

We demonstrate the possibility of selecting antibodies against the PC using the described selection strategy. We show that one of the selected antibodies, the C3 antibody, had a functional effect on PC behavior when applied in two different in vitro assays and we detect the antigen recognized by this antibody by mass spectrometry.

2 | MATERIAL AND METHODS

2.1 | Microcapillary surface modification

A glass capillary (MBB-FP-M-0, Origio, Maaloev, Denmark) was attached to a brass straight-arm needle holder (MINJ-4, TriTech Research, Los Angeles, CA, USA) and cleaned by withdrawing chromic-sulfuric acid solution into the capillary and subsequent incubation of the capillary immersed in the solution overnight. The capillary was flushed and rinsed in deionized distilled water (DDW), air-dried and subsequently incubated for 3 hours in a silanization solution containing 2% dimethyldichlorosilane in 1,1,1-trichloroethane (Sigma-Aldrich, Brøndby, Denmark). The capillary was rinsed in DDW, air-dried, and immersed in a 1 mg/mL solution of Pluronic F127 (PF127) surfactant (Sigma-Aldrich) dissolved in DDW. Surface-treated capillaries were stored in the PF127 solution and rinsed with DDW just prior to the time of use.

2.2 | Phage antibody selection

Human brain vascular pericytes (HBVP) (Sciencell Research Laboratories, Carlsbad, CA, USA), HMEC-1 (ATCC, Wesel, Germany), human aortic vascular smooth muscle cells (VSMC),[36] and ASF-2 fibroblasts (adult skin fibroblast)[37] were grown in pericyte medium (Sciencell), EGM medium (Lonza, Vallensbæk, Denmark), VSMC medium, and ASF-2 medium (DMEM, with 10% FBS and penicillin/streptomycin), respectively. Cell cultivation was performed at 37°C, 5% CO_2, and 95% humidity. HBVP were seeded in a Nunc Up-Cell dish
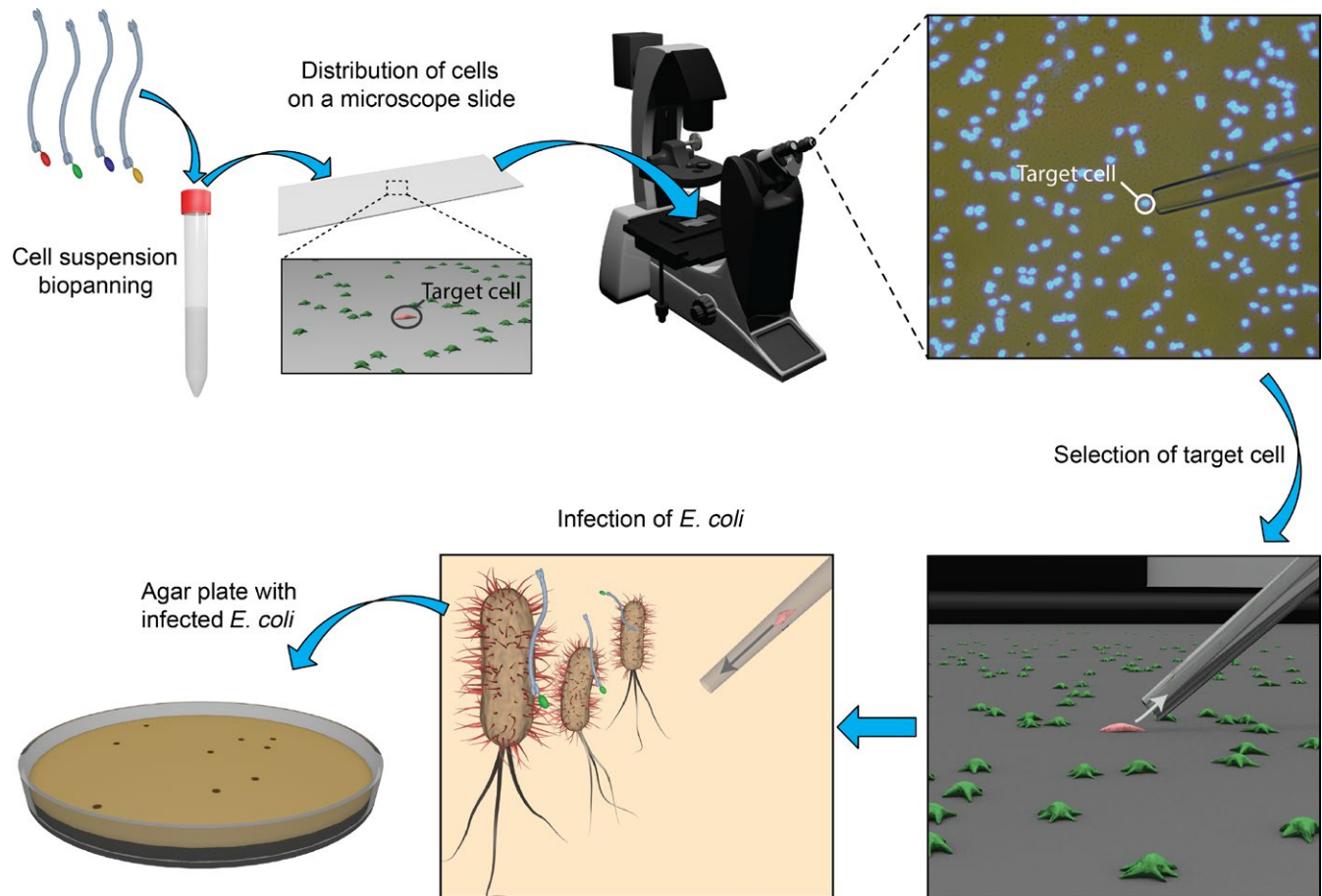
FIGURE 1 Method for selection of antibodies by targeting only single cells. The selection process is performed in solution, and the few target cells are subsequently identified under a microscope. The target cells are picked using in vitro fertilization equipment, and the antibody-phages bound to the cell are treated with trypsin prior to infection of *E. coli*. The phage particles carry an antibiotic resistance gene. Hence, only infected bacteria will give rise to colonies on the selective agar plate

(Thermo Scientific, Hvidovre, Denmark), with a temperature responsive nano-coating, for non-enzymatic harvesting of adherent cells to preserve surface antigens. The detached cells were harvested by placing the Up-Cell dish at room temperature for 20 min, and spun down at 800 g, 6 min, washed once in PBS, and then fixed for 10 min at room temperature in 2% PFA. The HBVP cells were then stained with phalloidin (Alexa Fluor 568 phalloidin, Thermo Scientific), and 100 cells were spiked into a population of at least 10^6 background cells (HBVP, HMEC-1, VSMC, and ASF-2). This cell suspension was incubated with 10^{12} phages (Predator Heavy Domain Antibody Library[38]) in 8 mL PBS containing 2% Marvel dried skimmed milk powder (MPBS) in a 15- mL centrifuge tube. The selection suspension was incubated for 2 hours at gentle rotation on an Intelli-Mixer at room temperature. Non-binding phage antibodies were removed by washing five times in PBS (centrifugation at 800 g for 6 min and resuspending the cell pellet in fresh PBS). After the last wash, the cells were resuspended in PBS containing DAPI (1:1000) (Thermofisher Scientific, Waltham, MA, USA). A small volume of the cell suspension was distributed on a poly-L-lysine coated microscope slide. The phalloidin stained PCs were identified under a microscope and specifically harvested by aspiration into a glass capillary (modified as described above) positioned by a

micromanipulation stage (Narishige, Model MM-188, Nikon, Tokyo, Japan). The picked cells (with bound phage) were eluted into microcentrifuge tubes and incubated with trypsin from Bovine pancreas (Sigma-Aldrich) (final concentration of 1 mg/mL) for 20 min at 37°C to reduce background of non-displaying phages.[35,39] The phages were used for infection into XL1-Blue and plated on a selective agar plate.

2.3 | Expression and purification of soluble antibodies in Leishmania tarentolae T7-TR

Sub-cloning, expression, and purification of selected domain antibodies fused to the Fc-region of rabbit IgG were conducted as previously described.[40] Antibodies secreted to the medium were ammonium sulfate precipitated by addition of ammonium sulfate to 30% W/V and the pellet resuspended in protein A binding buffer and purified on a protein A HP spinTrap column (GE Healthcare, Brøndby, Denmark) according to the manufacturer's protocol. Antibody purity and successful incorporation of the rabbit Fc-region were analyzed by means of SDS-PAGE and Western immunoblotting. Purified antibody concentration was measured at 280 nm on a Nanodrop 1000 spectrophotometer (Thermo Scientific).

2.4 | Whole-cell Enzyme-linked immunosorbent assay (ELISA)

For whole-cell ELISA, 10.000 HBVP, mouse brain vascular pericytes (MBVP),[41] VSMC, and HMEC-1 cells were seeded per well in a 96-well tissue culture plate and left in the incubator overnight for attachment. The cells were rinsed with DPBS and fixed for 15 min at room temperature in 3% paraformaldehyde-PBS (3% PFA-PBS). The cells were then washed with PBS and blocked in 2% MPBS for 1 h at room temperature. Incubation with primary antibody, C3 (20 µg/mL), was carried out for 1 hour at room temperature before washing 3 × 5 min in PBS-T. Secondary HRP-conjugated antibody, swine anti-rabbit HRP (Dako, Glostrup, Denmark), was applied and incubated for 1 hour at room temperature. The wells were washed, and the ELISA developed using TMB substrate solution (Sigma-Aldrich). The chromogenic reactions were terminated by addition of 1M H_2SO_4 and absorbances read at 450 nm (corrected with the reference wavelength 655 nm) using a microplate reader (Bio-Rad, Hercules, CA, USA). To account for well-to-well variation of cell number, Janus Green Whole-Cell Stain (Thermo Scientific) was used according to manufacturer's protocol to normalize the absorbance values (HRP activity).

2.5 | ELISA

Fibronectin specificity of the C3 antibody was tested by ELISA in 96-well flat bottomed Maxi-Sorp plates (Nunc, Roskilde, Denmark). The antigens, FN and alpha3 (proteasome subunit), were coated at a concentration of 2 µg/mL overnight at 4°C. The wells were then rinsed in PBS and blocked in 2% MPBS for 1 hour at room temperature. The blocking solution was discarded, and the C3, D4,[30] and A2 (2-5 µg/mL) antibodies were added to the wells and incubated for 1 hour at room temperature. The wells were washed 3 × 5 min in PBS-T before addition of swine anti-rabbit HRP (diluted 1:300) (Dako, cat nr. P0217, Glostrup, Denmark) secondary antibody for 1 hour at room temperature and subsequently washed and developed as described above.

2.6 | Immunoprecipitation and mass spectrometry

Three milligram Dynabeads Protein A suspension (Thermofisher Scientific) was prepared according to manufacturer's protocol and incubated for 30 min at room temperature with 200 µL antibody at a concentration of 200 µg/mL diluted in PBS. The beads were separated from the supernatant by magnetic sorting and washed three times in PBS-T. Bound antibody was then cross-linked to the beads using BS3 (bis(sulfosuccinimidyl)suberate) (Thermo Scientific) according to manufacturer's protocol. Antibody was mixed with approximately 50-fold molecular excess of BS3 (0.25 mM) in conjugation buffer and incubated for 30 min at room temperature, before quenching the cross-linking in quenching buffer for 15 min at room temperature. The beads were then washed three times in PBS-T and incubated with HBVP-conditioned medium for 1 hour at room temperature. The beads were washed three times in PBS-T, resuspended in 50 µL SDS sample buffer

(Bio-Rad, København Ø, Denmark), and heated at 95°C for 5 min to release the antigen. The antigen containing supernatant was cleared of beads by magnetic sorting, separated by SDS-PAGE, and proteins visualized by coomassie brilliant blue R-250 staining solution (Bio-Rad). The protein band was excised and prepared for in-gel digestion using porcine trypsin (Promega, Nacka, Sweden). The generated peptides were isolated and desalted using reversed-phase microcolumns (StageTips, C18; Thermo Fischer Scientific) and eluted directly onto a MALDI target plate using α-cyano-4-hydroxyciannamic acid in 70% acetonitrile and 0.1% trifluoroacetic acid (4 mg/mL). Peptides were subsequently analyzed using an Autoflex Smartbeam III instrument (Bruker, Billerica, MA, USA) calibrated using a peptide mixture containing seven calibrants (PepMix; Bruker). The acquired spectra were annotated using FlexAnalysis (v3.3) and interrogated by peptide mass fingerprinting using the Mascot search engine and the Swiss-Prot database (version 2015_04). Propionylation of cysteine residues was set as a fixed modification and the oxidation of methionine residues as a variable modification. One missed cleavage was allowed and the peptide mass tolerance set to 50 ppm. Protein identification was verified by manual inspection of datasets.

2.7 | Immunohistochemistry

Histological sections from three human eyes without any signs of ocular pathology were studied. The tissue had previously been embedded in paraffin, and four microns of histological sections had been sampled during autopsy at Aarhus University Hospital. The employment of this tissue was approved by the Regional Scientific Ethics Committee (File number 1-10-72-299-12). The sections were placed at 60°C for 15 min and then deparaffinized in HistoChoice (Sigma-Aldrich) for 2 × 5 min and then 1:1 HistoChoice (Sigma-Aldrich) and 99% ethanol for 5 min. The sections were rehydrated in series of ethanol solutions with concentrations of: 99%, 99%, 99%, 96%, 96%, 70%, and 50%. The sections were immersed in tap water, and antigen retrieval was carried out using BD retrievagen (BD Bioscience, San Jose, CA, USA) according to manufacturer's protocol before equilibration in TBS. The sections were then blocked in 2% BSA-TBS with 10% goat serum for 1 hour at room temperature before addition of primary antibody diluted in 2% BSA-TBS (C3, 20 µg/mL; anti-alpha smooth muscle actin [α-SMA] [Clone 1A4, DAKO], 10 µg/mL) overnight at 4°C. Non-bound primary antibody was washed away with TBS for 3 × 5 min, and fluorescently marked secondary antibody was applied for 1 hour at room temperature (goat anti-rabbit Alexa 488 [Invitrogen, Carlsbad, CA, USA] and goat anti-mouse Alexa 546 [Invitrogen] at 1:100 dilution in 2% BSA-TBS). The sections were washed in TBS and mounted with VECTASHIELD including DAPI (Vector Laboratories, Burlingame, CA, USA). Fluorescent images were obtained using a Leica DMI3000 B inverted microscope (Leica Microsystems, Wetzlar, Germany).

Human brain sections from the frontal cortex were supplied by Professor Claudio Franceschi, University of Bologna, Italy.[42] The tissue was embedded in OCT cryoprotectant and sampled in 10 microns sections on a cryostat. Cryo sections were left at room temperature for

5 min. and then blocked for 1 hour at room temperature in 2% BSA-TBS with 10% goat serum (Sigma-Aldrich). The staining procedure was carried out as above except a different set of primary antibodies were applied C3, 20 μg/mL; anti NG2, 10 μg/mL (Millipore, Hellerup, Denmark); Ulec Europaeus Agglutinin I, Vector Laboratories, 1:100 dilution (Vector Laboratories). Secondary antibodies were as follows: 1:100 dilution of goat anti-rabbit Alexa 546 (Invitrogen), 1:200 dilution of Streptavidin Alexa 488 (Invitrogen). For C3 and NG2 stainings, the images were obtained with a Leica DMI3000 B inverted microscope. For the C3 and UAEI, co-staining image stacks were obtained with a Zeiss LSM 780 confocal microscope (Zeiss, Oberkochen, Germany). All images were background subtracted and contrast stretched in ImageJ.

2.8 | Immunocytochemistry

For immunostaining, 10.000 HBVP cells were seeded in an ibiTreat μ-Slide VI 0.4 (Ibidi, Martinsried, Germany) and incubated (37°C, 5% CO_2 and 95% humidity) for 2 and 6 hours, respectively. The cells were rinsed once in PBS, fixed in 4% PFA for 10 min, blocked in DMEM with 10% FBS, and incubated with 20 μg/mL of purified antibody diluted in blocking solution for 1 hour at room temperature. When co-staining with phalloidin, cells were additionally permeabilized with 0.2% Triton X-100 (Sigma-Aldrich) for 10 min prior to incubation with primary antibody. The cells were washed and incubated with Alexa Fluor 488-conjugated goat anti-rabbit IgG (Invitrogen) for 1 hour at room temperature for detection of primary antibody. Cell nuclei were counter stained with DAPI (VECTASHIELD Mounting Medium, Vector Laboratories), and fluorescent images were obtained using a Leica DMI3000 B inverted microscope (Leica Microsystems).

2.9 | Tube formation assay using HBVP and HBMEC

Several optimization steps were performed to determine time point of data acquisition, cell density, and cell-to-cell ratio to provide comparable and reproducible data.

The tube formation assay was carried out according to the IBIDI protocol. Matrigel Growth Factor Reduced Basement Membrane Matrix (Corning, Corning, NY, USA) was thawed on ice at 4°C overnight. A μ-Slide Angiogenesis slide (Ibidi) was placed on a cold rack in the flow bench. 10 μL of thawed Matrigel was added to each of the inner wells with precooled tips. Subsequently, the slide was incubated (37°C, 5% CO_2 and 95% humidity) for 30 min to polymerize. Different concentrations of antibody were added to individual cell suspensions each containing a total of 6000 cells in a 1:1 ratio of HBVP and HBMEC. After Matrigel polymerization, the antibody-cell suspensions were added to each well (in a volume of 50 μL) and the slide incubated at 37°C, 5% CO_2 and 95% humidity. Each biological replicate was made in technical replicates of five, and images of emerging tubes were captured at different time points (3, 6, and 9 hours) by phase contrast microscopy using a 4 × objective, Zeiss Axiocam ERc 5s (Carl Zeiss Microscopy, Oberkochen, Germany) (Figs. S3 and S4). The images were processed by ImageJ, and total tube length was quantified by the Angiogenesis Analyzer plugin.[43]

2.10 | Scratch wound assay

HBVP were seeded in a 12-well plate at 10^5 cells/well and grown to a confluent monolayer overnight. Two intersecting straight "scratches" were made with a p200 pipet tip. Cell medium was aspirated, and the cells were rinsed in DPBS to remove cell debris. Cell medium with an antibody concentration of 50 μg/mL was then added to the wells with PBS diluted medium used as a control. Each biological replicate was made in technical replicates of three. Images were captured at different time points (2, 4, 6, 8, 10, 12, and 24 hours) with a Zeiss Axiocam ERc 5s (Carl Zeiss Microscopy). Each scratch wound area was analyzed by measuring the cell-free area using ImageJ's freehand selection. The dataset was blinded and scored independently by two investigators.

2.11 | Statistical analysis of tube formation assay and scratch wound assay

Data were shown as the mean ± SEM and statistically compared by a parametric, unpaired Student's t-test. The statistical analysis was performed by statistical software (GraphPad Prism 6.0, GraphPad Software, Inc., La Jolla, CA, USA).

3 | RESULTS

3.1 | Selections and screening

For selection of antibodies against the PC, primary human brain vascular pericytes (HBVP) were used as target cells. PC morphology visualized by phalloidin-marked F-actin and positive staining for the PC marker PDGFR-beta (Figure 2) in combination with previous reported phenotypic validation (positive for α-SMA, NG2, CD13, CD73, and CD105 and negative for CD31, CD34, and CD45)[44] verified PC identity. The phage antibody selections were performed by means of cell suspension biopanning followed by selection as outlined in Figure. 1. Multiple selections were performed in parallel using the "Predator" single-domain phage antibody library.[38] Typically, using this method, an output of 1-10 antibody clones per target cell aspirated can be expected. In the selection, eight PCs were specifically picked from the suspension of background cells and resulted in the recovery of 12 antibody clones. Dilution series ELISA was performed to screen and prioritize the antibody clones for further characterization (Fig. S1). The antibody clone, C3, was selected for further characterization.

3.2 | Antibody characterization

The single-domain antibody gene for C3 was sub-cloned into pMJ-LEXSY-rFc,[40] containing the rabbit IgG Fc-encoding region (hinge region and CH2-CH3 domains) and expressed in Leishmania tarentolae (TR/T7). The purity was confirmed by SDS-PAGE, while the presence of the Fc-region was verified by Western immunoblotting (Fig. S2).

Whole-cell ELISA against cell types observed adjacent to the pericyte in vivo confirmed the specificity of the C3 antibody. An
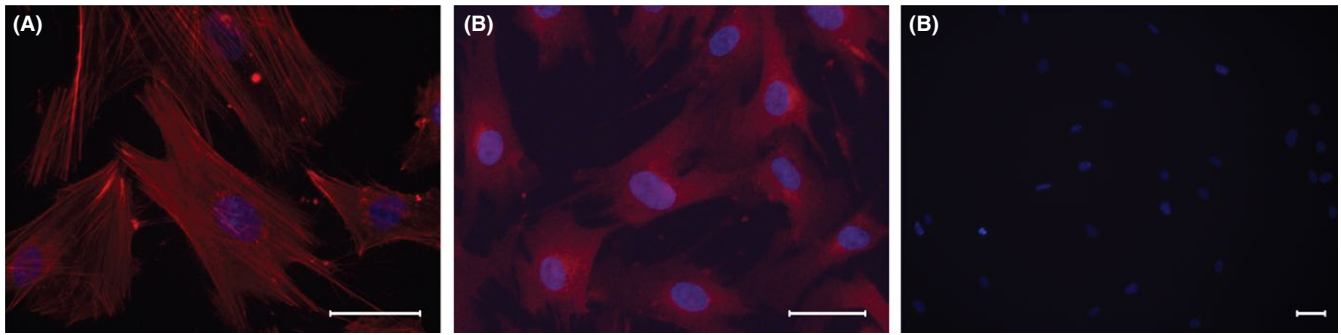
FIGURE 2 Pericyte morphology visualized by phalloidin-marked F-actin and PDGFR-beta. Staining of HBVP with Alexa Fluor 568 phalloidin (A), with primary rabbit anti-PDGFR-β antibody and secondary goat anti-rabbit Alexa Fluor 546-conjugated antibody (B) and control staining with secondary antibody only. Cell nuclei were stained with DAPI (blue). Scale bars=40 μm
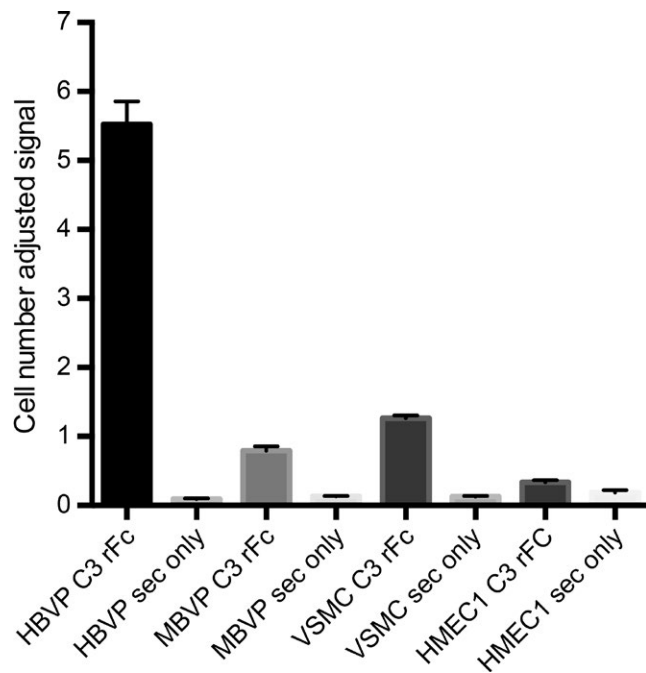
FIGURE 3 Determination of antigen expression level by whole-cell ELISA. Primary antibody, C3-rFc, was applied on human brain vascular pericytes (HBVP), mouse brain vascular pericytes (MBVP), human vascular smooth muscle cells (VSMC) and a human microvascular endothelial cell line (HMEC-1). C3-rFC was detected with a secondary swine anti-rabbit HRP-conjugated antibody

approximately 10-fold binding preference for PC to EC was observed, whereas a fourfold binding preference for PC to VSMC was observed (Figure 3). Furthermore, only slight cross-species reactivity between human and mouse was detected.

## 3.3 | Antigen identification

To assess antigen distribution, C3 was applied in immunocytochemistry. Fluorescent images taken at different time points after seeding of cultured PCs revealed a change in antigen distribution over time (Figure 4). Cell boundaries were visualized by F-actin marked with phalloidin (red). After 2 hours, the antigen was predominantly present intracellularly but after 10 hours, increased extracellular deposition of antigen was observed. This was especially evident when the cells were not permeabilized before immunostaining and hence only allowing extracellular access of the antibody.

As it was evident that large amounts of antigen were secreted by cultured PCs, antigen immunoprecipitation was performed on PC conditioned medium. Bound antigen was eluted and analyzed by SDS-PAGE. One clear band around 250 kDa was observed (Figure 5), which was excised, digested, and subsequently analyzed by mass spectrometry. With 42 peptide matches, the antigen was identified with high confidence (Mascot score = 264; sequence coverage: 12%) as fibronectin (FN) (Swiss-Prot accession number P02751).

3.4 | Antigen validation

Firstly, an ELISA experiment on purified FN was carried out to confirm the specificity of C3 (Figure 6). Along with two FN-specific antibodies, D4 (scFv)[30] and A2 (single domain-rFc), previously selected in our laboratory, C3 showed specific binding to FN with no cross-reactivity observed against milk proteins or a proteasomal subunit. Secondly, C3 was applied in immunohistochemistry on human retina and cerebral cortex sections (Figure 7). Intense perivascular staining was observed around the microvessels in the retina (Figure 7A,B). Furthermore, α-smooth muscle actin (α-SMA)-positive cells, a frequently used PC marker, were embedded in the C3 stained FN-containing matrix (Figure 7C). This is in line with the literature describing the PC as a mural cell embedded in the EC basement membrane. Although the retina sections exhibited excellent morphological preservation, it proved difficult to target PC and EC markers with commercial antibodies here—most likely because of the fixation technique used. In an attempt to preserve the epitope recognized, cerebral cortex tissue[42] was snapfrozen, cryo-sectioned, and only gently fixed. Although the morphology was clearly inferior compared to the retina sections, it was possible to target commonly used EC and PC markers in this set-up (Figure 7E-I). As expected, C3 showed a perivascular staining pattern abluminal to the endothelial cells marked by Ulex Europaeus Agglutinin I (UAE I). Furthermore, the C3 antibody showed an identical staining pattern to NG2 chondroitin sulfate proteoglycan-positive cells. In this set-up, NG2 appeared to be the best commercial marker for quiescent PCs compared to PDGFR-beta and alpha-SMA (data not shown).
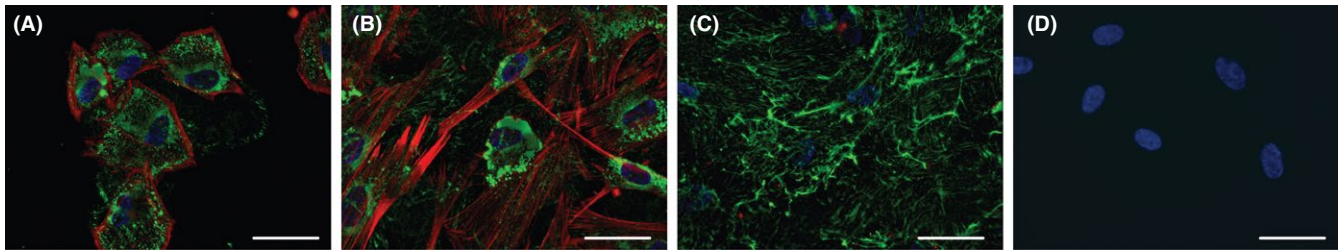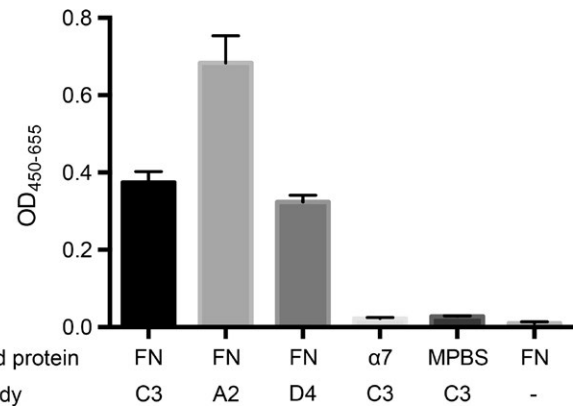
FIGURE 4 The C3 antibody targets an extracellular antigen secreted by the pericyte. HBVP stained with Alexa Fluor 568 phalloidin (red) and C3-rFC detected with a secondary goat anti-rabbit Alexa Fluor 488-conjugated antibody (green). Cell nuclei are stained with DAPI (blue). HBVP were permeabilized, fixed in PFA, and stained 2 hours (A) or 10 hours (B) after cell seeding to visualize antigen presentation at different time points. Non-permeabilized HBVP stained before fixation 10 hours after cell seeding (C). Control staining of HBVP with secondary antibody only (D). Scale bar=40 μm
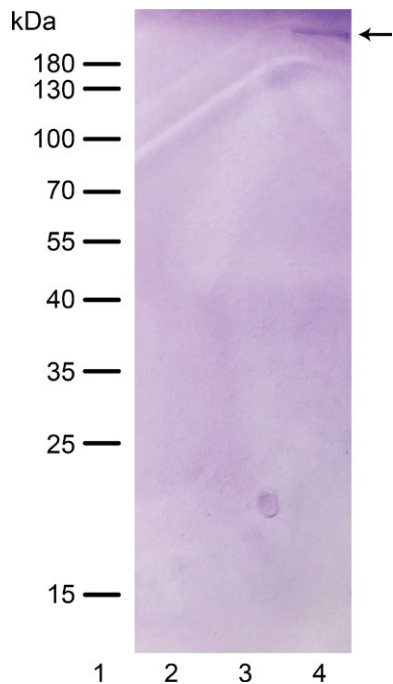
FIGURE 5 Immunoprecipitation of fibronectin by the C3 antibody. C3-rFc was cross-linked to protein A Dynabeads and incubated with HBVP-conditioned medium. Captured antigen was released, separated by SDS-PAGE, and visualized by coomassie staining. 1: Marker, 2: C3-rFc cross-linked to protein A Dynabeads incubated with PBS, 3: C3-rFc cross-linked to protein A Dynabeads incubated with unconditioned medium, 4: C3-rFc cross-linked to protein A Dynabeads incubated with conditioned medium. Only one target protein was captured by C3-rFc (arrow)

FIGURE 6 Validation of antibody-fibronectin binding by ELISA. C3-rFc was tested together with two previously isolated anti-FN antibodies (A2 and D4) on purified FN and detected with a secondary swine anti-rabbit HRP-conjugated antibody. The proteasomal subunit α7 and skimmed milk powder in PBS (MPBS) was used as negative controls. A negative control for non-specific binding of secondary antibody to FN was performed by omitting primary antibody

3.5 | In vitro wound healing assay

Initially, the physiological effect of the C3-FN interaction was investigated in a scratch wound assay using cultured PCs to observe effect on cell migration. Interestingly, after an initial 20% closing of the wound, the C3 antibody completely inhibited PC migration from 4 hours and onwards, while the isotype control (A2-rFc) and medium-only control closed the wound approximately linear (Figure 8). As the cognate antigen of A2-rFc is also FN, it is indicated that blockage of a unique FN epitope by the C3 antibody had a potent anti-migratory effect on PCs.

3.6 | In vitro angiogenesis tube formation assay

The effect of FN blockage by the C3 antibody was analyzed in an in vitro PC/EC co-culture tube formation assay. A preliminary experiment revealed that the PC in itself only had limited tube formation ability, while ECs readily formed tubes. Moreover, a 1:1 ratio of PC to EC provided optimal conditions for tube formation (Fig. S4), corresponding well with the ratio observed in vivo in the brain and retina. After a 3- hour sprouting period, a 25% increase in tube length was observed compared to controls and 50% compared to the anti-angiogenic antibody L36[45] (Figure 9). After 6 and 9 hours of sprouting, the differences were less pronounced.

4 | DISCUSSION

In this study, a novel phage display selection method was developed for the selection of antibodies against the PC, with the prime focus on identifying novel therapeutic candidates with regulatory effects on PC function. However, the described selection method can easily
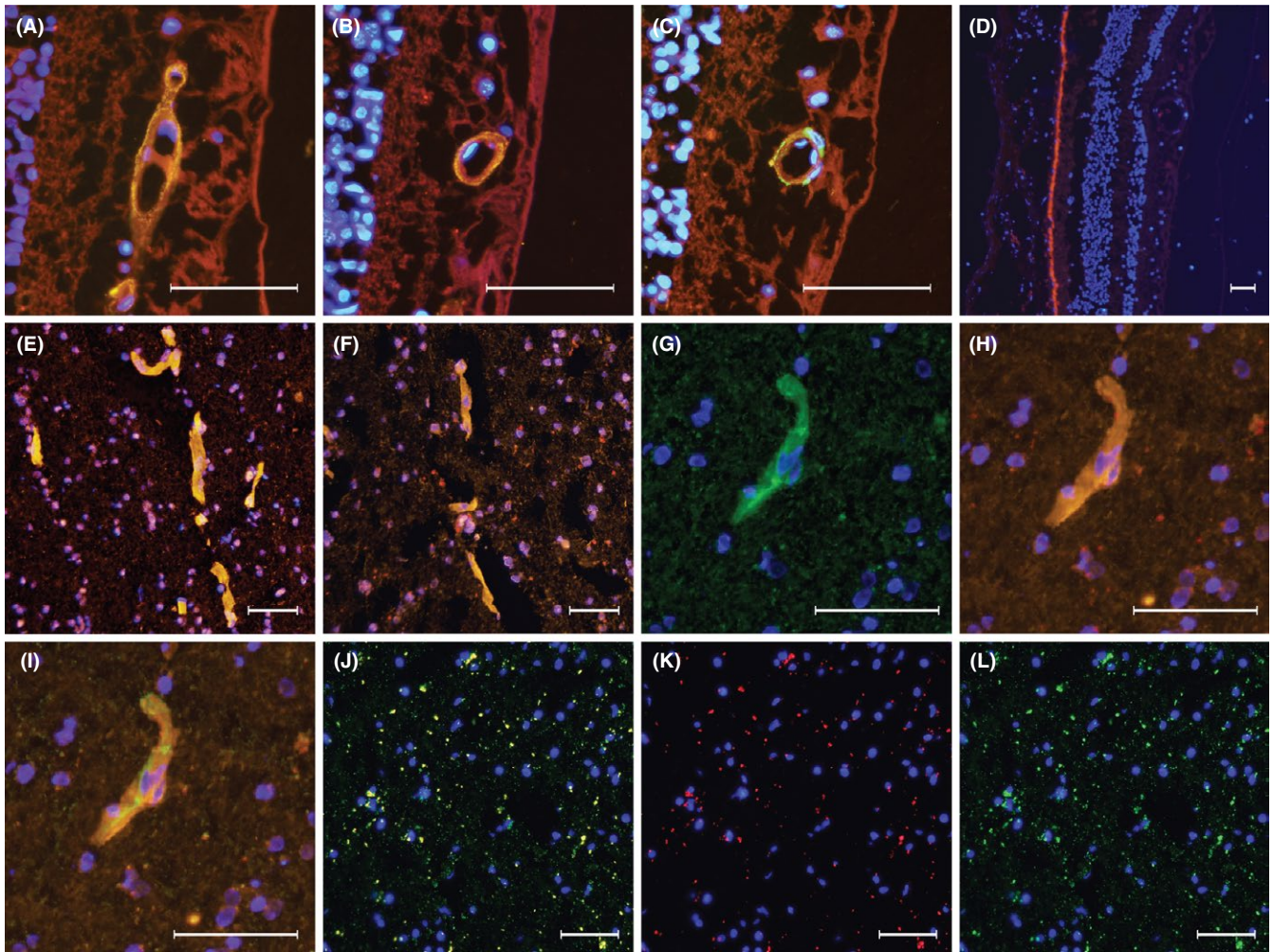
FIGURE 7 The C3 antibody showing staining around the microvessels in human retina and cerebral cortex. A-C: Human retina stained with the C3 antibody (orange). An intense staining around the microvessels was observed (A+B). Alpha-SMA-positive cells (green) were observed embedded in the C3 antibody staining pattern (C). D: control staining on retina with secondary antibody only. E-L: Immunostaining on human cerebral cortex. E: NG2-positive cells (orange). F: C3 antibody staining (orange) observed along the microvasculature. G-I: Co-staining with the C3 antibody (orange) and UAEI, a marker of endothelial cells in the microvasculature (green). C3 staining was observed on the abluminal side of endothelial cells. J-L: Control staining with secondary antibody only. A-L: Cell nuclei were stained with DAPI (blue). Scale bar=50 μm
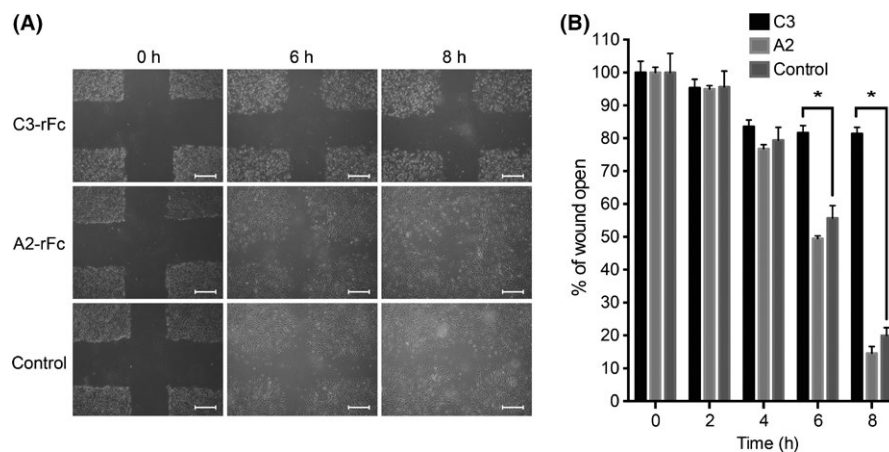
FIGURE 8 Effect of C3-rFc on scratch wound closure rate in pericyte cell cultures. Migration of cells into the cell-free area was measured at time intervals of 2 hours during the cultivation of HBVP with A2 (anti-FN antibody), C3 and medium only (control). Pictures of the cell migration at 0, 6 and 8 hours are presented (A). Data from three separate scratch assays were aggregated and % of open wound (area not occupied by cells) represented in the column chart (B). C3-treated pericytes showed inhibition of migration after 6 hours compared to the control (no antibody) and A2 (B). Values are expressed as the means ± SEM (n = 3). *Statistical significance: $P < 0.05$
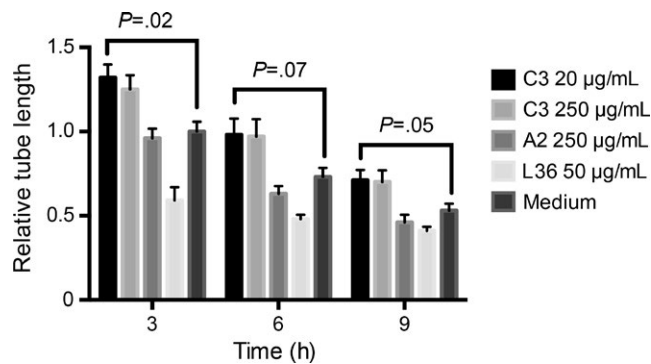
FIGURE 9 C3-rFc increased in vitro tube formation in a pericyte and endothelial cell Matrigel co-culture. The total tube lengths were quantified during the cultivation (3, 6 and 9 hours) of a 1:1 ratio of HBVP and HBMEC incubated with L36 (anti-angiogenic antibody), A2 (anti-FN antibody) and C3 in two different concentrations. A significant pro-angiogenic effect was observed after 3 hours, with a 30% increase in tube lengths observed. Values are expressed as the means ± SEM (n = 4), and P-values are given on the chart

be implemented for isolation of antibodies against other cell types. We have successfully selected antibodies against K562 leukemia cells spiked into a background of another leukemia cell line (1301 cell) (Figs S5 and S6). Additionally, the method has been applied for isolation of antibodies specific for circulating tumor cells (CTCs) in colorectal cancer patients (unpublished results). The low number of output clones and the relatively high frequency of antibodies with binding preference for the cell type of interest reduce the workload of subsequent antibody screenings. This is particularly relevant when the cell material for screening is scarce (eg primary cell lines). Depletion strategies for directing antibody selections toward relevant antigens or epitopes are widely used. It is generally accepted that such strategies can increase the representation of antibodies against desired epitopes on purified protein by competitive de-selection with a related antigen carrying a common epitope.[46] However, for selections on complex targets such as cell surface antigens, the efficiency of library depletion steps is more difficult to assess. A few studies have reported reduction in cross-reactivity of fourfold to 10-fold to blood cells in a selection against colorectal cancer cells,[32] and complete depletion of binders to red blood cells after four rounds of extensive subtraction of antiserum from a mouse immunized with a prostate cancer cell line.[33] In the presented work, a synthetic antibody library was used for isolation of PC-specific antibodies. This library has previously been applied in a direct cell panning procedure against PCs with only limited success.[38] Although a considered fraction of the initially screened 384 clones had promising binding signal on PCs compared to medium, most of these clones revealed to be unspecific in a second screening against HMEC-1, ASF-2, and VSMCs. As a consequence, only the two presented antibody clones (M3H12 and M4E7) showed to be specific for PCs.

For the antibody selection using the strategy presented here, cells neighboring the PC in vivo were used as background cells. From this, a panel of 12 antibodies targeting the PC was obtained and whole-cell ELISA was used to validate the specificity of these antibodies relative to adjacent cell types. From the selected antibodies, two clones (C3 and C8) showed binding preference for PCs with C3 being the most PC-specific candidate. Interestingly, C3 also revealed an approximately sixfold higher binding signal on HBVP compared to MBVP. The increased signal on HBVP compared to MBVP indicated that the epitope is either poorly conserved between mouse and human, or, the antigen expression level is higher in human derived cultured PCs. VSMC are generally considered to be closely related to PCs.[47] Hence, identification of antigens uniquely expressed by either of these cell types is a challenging task. Furthermore, as the PC has been suggested to have stem cell like characteristics, a certain degree of heterogeneity in the in vitro cultivated PCs and VSMCs should be expected. The fourfold change in binding observed between the two cells types could possibly be a result of cellular drift in the cultures, used for ELISA, toward similar phenotypes. Consequently, although the C3 antibody showed moderate binding signal to VSMC, it was chosen for further analysis. In vitro cultivation of cells isolated from tissue is known to provoke a change in gene expression,[48] it is therefore difficult to conclude to what extend a fourfold increase of binding of C3 to PCs compared the VSMCs translates to specificity observed in the tissue.

By comparing the C3-rFc staining patterns on HBVP after 2 hours and 10 hours of cultivation, a change in antigen location was observed. After 2 hours, the C3-rFc staining was primarily located intracellularly, whereas after 10 hours increased extracellular staining was detected. Identification of FN as the cognate antigen correlated well with the staining observed on human retina and brain sections. Intense staining was observed around the blood vessels, abluminal to the endothelial cell, and a similar staining pattern was observed with the commonly used PC marker NG2. Furthermore, another commonly used PC marker, alpha-SMA, was applied. As expected, alpha-SMA-positive cells were located within the C3 stained FN-containing matrix in retina sections. This is consistent with the presence of FN in the shared basement membrane between EC and PC, in which the PC is embedded.

Fibronectin is an extracellular matrix protein secreted as a soluble dimer by various cell types, including PCs,[49,50] and it is found only in organisms with an endothelium-lined vasculature. PCs have been shown to express ten times more FN than endothelial cells giving an indication that the PC is an important producer of secreted FN in the microvessels.[51] FN is a highly complex molecule with multiple binding sites for other ECM proteins, growth factors, and cells surface receptors.[52] FN is encoded by a single gene and exists in several possible monomeric isoforms produced by alternative splicing. Thus, different isoforms of FN can be expressed in a tissue-dependent and cell type-specific manner.[53] The alternatively spliced extra-domain A (EIIIA) and extra-domain B (EIIIB) have been observed to be elevated during vascular development, vascular remodeling, and in pathological conditions such as cancer and atherosclerosis.[54] Functionally, FN is essential for blood vessel vasculogenesis, angiogenesis, and homeostasis.[55–57] In the microvessels, FN is located between the EC and PC where the FN fibrillar and microfilament bundle arrangement in the ECM (adhesion plaques) serves to anchor the PC to the EC.[49] In the formation of vascular networks, these PC-EC interactions are positively and negatively

modulated, regulating cell adhesion, cell migration, and organization of the cytoskeleton.[49,56–58] The cell integrin α4β1 is believed to be of special importance for PC interaction with FN. In primary PCs negative for α4, α4β1 integrin adhesion was affected.[59] Furthermore, α4 integrin-deficient mice embryos displayed increased microvessel size in the cranial regions, reduced PC coverage and abnormal distribution. α4 integrin expression was only observed in PCs and not ECs of the developing vasculature, indicating that α4β1 integrin interaction with FN is important for PC attachment and migration in developing vessels.[60]

In recent years, FN has been suggested as an interesting drug target, as the role of the tumor stroma and its ECM components in tumor growth and progression is becoming evident. Furthermore, the abundance and accessibility of the ECM may allow for efficient delivery of antibodies to tumor environment. Certain isoforms of FN have been shown to accumulate around the neovasculature in the tumor environment.[61] In the tumor neovasculature, accumulation of oncofetal isoforms of FN has been observed. Here, the EIIIA and EIIIB are of special interest and two monoclonal antibodies targeting either form have been selected by phage display: F8 and L19, respectively.[62] The alternatively spliced EIIIB was validated as an oncofetal antigen highly specific for tumor growth and angiogenesis and injection of labeled L19 showed selective uptake in tumor lesions. In addition, L19 was successfully armed by conjugation to different cytokines for delivering potent cytotoxic effects to the tumor environment.[61,63] Interestingly, the number of pericytes surrounding the tumor vessels may correlate with the expression level of FN. Tumor vessels with high abundance of FN seems to have a thick layer of PCs attached, while tumor vessels with no FN only have a single layer or no PCs attached at all.[49] Consequently, an impairment of the PC-FN interaction could impact vascular development and stabilization of the tumor vasculature and serve as an attractive target in cancer therapy.[64]

The potential functional effect of the C3 antibody was therefore investigated in in vitro wound healing and tube formation assays. After 6 hours, C3-FN interaction was found to inhibit PC migration completely in a scratch wound assay. In the tube formation assay, C3 had a significant pro-angiogenic effect after 3 hours, with a 25% increase in total tube length. These results strongly suggest that C3 block a functional interaction site on FN secreted by the PC. The greatest impact was observed on PC migration. As the tube formation assay performed here involve both PCs and ECs in a co-culture system, the lack of migration of the PCs could potentially explain the increased total tube length measured in the initiation process of tube formation, that is, as the PCs are prevented from migration, they are prevented from taking part in vessel stabilization. In the initiation of angiogenesis, ECs are believed to be stimulated by angiogenic factors allowing the EC to invade the surrounding extracellular matrix.[65] Vascular active ECs at the tip of an angiogenic sprout secretes PDGFB as a dimer, which interacts with the heparin sulfate proteoglycans of the extracellular matrix for local retention.[14] This concentration gradient attracts PDGFR-β-positive PCs to the newly formed vessel and contact introduces further maturation through different transduction pathways including TGF-beta signaling and angiopoietin-1/2—Tie-2.[15,47,58,66] It can be hypothesized that the blockade of the PC-FN interaction by the C3 antibody prevents PCs from migration along the PDGFR-b gradient, thus allowing ECs forming tubes with an increased length, due to lack of PC stabilization.

The extra tube formation observed may mimic the uncontrolled blood vessel sprouting observed in various cancers where PC loss or dysfunction is observed.[67,68] In this context, the C3 antibody could have therapeutic benefit in cancers where overexpression of FN and increased PC coverage are observed by blocking the attachment of PCs to the tumor vasculature.

In conclusion, we successfully demonstrated the possibility of selecting functional antibodies against the PC using the selection strategy outlined herein. We show that an antibody, C3, targets a FN epitope important for pericyte interaction and functionality. This FN epitope could serve as a potential interesting drug target in the development of novel vascular therapeutics.

PERSPECTIVES

The ability to specifically and effectively target different components of the vasculature is instrumental to normalize a diseased vasculature during a pathological state. Therefore, we have developed a novel antibody single-cell selection method, which can be implemented in drug discovery as a fast and efficient selection procedure of functional therapeutic antibodies. With an antibody obtained by the described selection strategy, we show the possibility of modulating pericyte behavior by affecting a PC interaction with ECM FN. Mapping this PC-FN interaction, and other interactions between vascular cells and the ECM, will provide interesting new drug target candidates.

REFERENCES

1. Armulik A, Betsholtz C. Role of pericytes in vascular biology. In: Hammes H-PP, porta M. eds. *Experimental Approaches to Diabetic Retinopathy* Vol. 20. Basel: Karger; 2010: 194-202.
2. Krueger M, Bechmann I. CNS pericytes: Concepts, misconceptions, and a way out. *Glia*. 2010;58:1-10.
3. Hogan MJ, Feeney L. The ultrastructure of the retinal blood vessels. I. the large vessels. *J Ultrastruct Res*. 1963;39:10-28.
4. Armulik A, Genové G, Betsholtz C. Pericytes: Developmental, physiological, and pathological perspectives, problems, and promises. *Dev Cell*. 2011;21:193-215.
5. Diaz-Flores L, Gutierrez R, Madrid JF, et al. Pericytes. morphofunction, interactions and pathology in a quiescent and activated mesenchymal cell niche. *Histol Histopathol*. 2009;24:909-969.
6. Mathiisen TM, Lehre KP, Danbolt NC, Ottersen OP. The perivascular astroglial sheath provides a complete covering of the brain microvessels: An electron microscopic 3D reconstruction. *Glia*. 2010;58:1094-1103.

7. Bobbie MW, Roy S, Trudeau K, Munger SJ, Simon AM, Roy S. Reduced connexin 43 expression and its effect on the development of vascular lesions in retinas of diabetic mice. *Invest Ophthalmol Vis Sci*. 2010;51:3758-3763.

8. Gerhardt H, Wolburg H, Redies C. N-cadherin mediates pericytic-endothelial interaction during brain angiogenesis in the chicken. *Dev Dyn*. 2000;218:472-479.

9. Winkler Ea, Bell RD, Zlokovic BV. Central nervous system pericytes in health and disease. *Nat Neurosci*. 2011;14:1398-1405.

10. Winkler EA, Bell RD, Zlokovic BV. Lack of Smad or Notch leads to a fatal game of brain pericyte hopscotch. *Dev Cell*. 2011;20:279-280.

11. Armulik A, Genové G, Mäe M, et al. Pericytes regulate the blood-brain barrier. *Nature*. 2010;468:557-561.

12. Bell RD, Winkler Ea, Sagare AP, et al. Pericytes control key neurovascular functions and neuronal phenotype in the adult brain and during brain aging. *Neuron*. 2010;68:409-427.

13. Daneman R, Zhou L, Kebede AA, Barres BA. Pericytes are required for blood-brain barrier integrity during embryogenesis. *Nature*. 2010;468:562-566.

14. Lindahl P, Johansson BR, Leveen P, Betsholtz C. Pericyte loss and microaneurysm formation in PDGF-B-deficient mice. *Science*. 1997;277:242-245.

15. Lindblom P, Gerhardt H, Liebner S, et al. Endothelial PDGF-B retention is required for proper investment of pericytes in the microvessel wall. *Genes Dev*. 2003;17:1835-1840.

16. Hammes HP, Feng Y, Pfister F, Brownlee M. Diabetic retinopathy: Targeting vasoregression. *Diabetes*. 2011;60:9-16.

17. Meng MB, Zaorsky NG, Deng L, et al. Pericytes: A double-edged sword in cancer therapy. *Future oncol*. 2015;11:169-179.

18. Quaegebeur A, Segura I, Carmeliet P. Pericytes: Blood-brain barrier safeguards against neurodegeneration?. *Neuron*. 2010;68:321-323.

19. Ribeiro AL, Okamoto OK. Combined effects of pericytes in the tumor microenvironment. *Stem Cells Int*. 2015;2015:868475.

20. Bradbury AR, Marks JD. Antibodies from phage antibody libraries. *J Immunol Methods*. 2004;290:29-49.

21. Lorenz HM. Technology evaluation: Adalimumab, Abbott laboratories. *Curr Opin Mol Ther*. 2002;4:185-190.

22. Sanchez-Martin D, Martinez-Torrecuadrada J, Teesalu T, et al. Proteasome activator complex PA28 identified as an accessible target in prostate cancer by in vivo selection of human antibodies. *Proc Natl Acad Sci USA*. 2013;110:13791-13796.

23. Paterson J, Webster CI. Exploiting transferrin receptor for delivering drugs across the blood-brain barrier. *Drug Discov Today Technol*. 2016;20:49-52.

24. Smith GP. Filamentous fusion phage: Novel expression vectors that display cloned antigens on the virion surface. *Science*. 1985;228:1315-1317.

25. Gao C, Mao S, Lo CH, Wirsching P, Lerner RA, Janda KD. Making artificial antibodies: A format for phage display of combinatorial heterodimeric arrays. *Proc Natl Acad Sci USA*. 1999;96:6025-6030.

26. Il'ichev AA, Minenkova OO, Tat'kov SI, et al. Production of a viable variant of the M13 phage with a foreign peptide inserted into the basic coat protein. *Dokl Akad Nauk SSSR*. 1989;307:481-483.

27. Jespers LS, Messens JH, De Keyser A, et al. Surface expression and ligand-based selection of cDNAs fused to filamentous phage gene VI. *Biotechnology (N Y)*. 1995;13:378-382.

28. Kang AS, Barbas CF, Janda KD, Benkovic SJ, Lerner RA. Linkage of recognition and replication functions by assembling combinatorial antibody Fab libraries along phage surfaces. *Proc Natl Acad Sci USA*. 1991;88:4363-4366.

29. Makowski L. Structural constraints on the display of foreign peptides on filamentous bacteriophages. *Gene*. 1993;128:5-11.

30. Jensen KB, Jensen ON, Ravn P, Clark BF, Kristensen P. Identification of keratinocyte-specific markers using phage display and mass spectrometry. *Mol Cell Proteomics*. 2003;2:61-69.

31. Even-Desrumeaux K, Nevoltris D, Lavaut M, et al. Masked selection: A straightforward and flexible approach for the selection of binders against specific epitopes and differentially expressed proteins by phage display. *Mol Cell Proteomics*. 2014;13:653-665.

32. Liebman MA, Williams BR, Daley KM, Sharon J. Generation and preliminary characterization of an antibody library with preferential reactivity to human colorectal cancer cells as compared to normal human blood cells. *Immunol Lett*. 2004;91:179-188.

33. Siva AC, Kirkland RE, Lin B, et al. Selection of anti-cancer antibodies from combinatorial libraries by whole-cell panning and stringent subtraction with human blood cells. *J Immunol Methods*. 2008;330:109-119.

34. Sørensen MD, Agerholm IE, Christensen B, Kølvraa S, Kristensen P. Microselection–affinity selecting antibodies against a single rare cell in a heterogeneous population. *J Cell Mol Med*. 2010;14:1953-1961.

35. Sørensen MD, Kristensen P. Selection of antibodies against a single rare cell present in a heterogeneous population using phage display. *Nat Protoc*. 2011;6:509-522.

36. Schultz K, Rasmussen LM, Ledet T. Expression levels and functional aspects of the hyaluronan receptor CD44. Effects of insulin, glucose, IGF-I, or growth hormone on human arterial smooth muscle cells. *Metabolism*. 2005;54:287-295.

37. Rattan SI, Sodagam L. Gerontomodulatory and youth-preserving effects of zeatin on human skin fibroblasts undergoing aging in vitro. *Rejuvenation Res*. 2005;8:46-57.

38. Mandrup OA, Friis NA, Lykkemark S, Just J, Kristensen P. A novel heavy domain antibody library with functionally optimized complementarity determining regions. *PLoS One*. 2013;8:e76834.

39. Kristensen P, Winter G. Proteolytic selection for protein folding using filamentous bacteriophages. *Fold Des*. 1998;3:321-328.

40. Jorgensen ML, Friis NA, Just J, Madsen P, Petersen SV, Kristensen P. Expression of single-chain variable fragments fused with the Fc-region of rabbit IgG in Leishmania tarentolae. *Microb Cell Fact*. 2014;13:9.

41. Thomsen MS, Birkelund S, Burkhart A, Stensballe A, Moos T. Synthesis and deposition of basement membrane proteins by primary brain capillary endothelial cells in a murine model of the blood-brain barrier. *J Neurochem*. 2016;140:741-754.

42. Mishto M, Bellavista E, Santoro A, et al. Immunoproteasome and LMP2 polymorphism in aged and Alzheimer's disease brains. *Neurobiol Aging*. 2006;27:54-66.

43. Carpentier G. ImageJ contribution: Angiogenesis Analyzer. In, edn, ImageJ News5 October 2012.

44. Guijarro-Munoz I, Compte M, Alvarez-Cienfuegos A, Alvarez-Vallina L, Sanz L. Lipopolysaccharide activates Toll-like receptor 4 (TLR4)-mediated NF-kappaB signaling pathway and proinflammatory response in human pericytes. *J Biol Chem*. 2014;289:2457-2468.

45. Sanz L, Kristensen P, Blanco B, et al. Single-chain antibody-based gene therapy: Inhibition of tumor growth by in situ production of phage-derived human antibody fragments blocking functionally active sites of cell-associated matrices. *Gene Ther*. 2002;9:1049-1053.

46. Parsons HL, Earnshaw JC, Wilton J, et al. Directing phage selections towards specific epitopes. *Protein Eng*. 1996;9:1043-1049.

47. Armulik A, Abramsson A, Betsholtz C. Endothelial/pericyte interactions. *Circ Res*. 2005;97:512-523.

48. Edfors F, Danielsson F, Hallstrom BM, et al. Gene-specific correlation of RNA and protein levels in human cells and tissues. *Mol Syst Biol*. 2016;12:883.

49. Astrof S, Hynes RO. Fibronectins in vascular morphogenesis. *Angiogenesis*. 2009;12:165-175.

50. Wierzbicka-Patynowski I, Schwarzbauer JE. The ins and outs of fibronectin matrix assembly. *J Cell Sci*. 2003;116:3269-3276.

51. Mandarino LJ, Sundarraj N, Finlayson J, Hassell HR. Regulation of fibronectin and laminin synthesis by retinal capillary endothelial cells and pericytes in vitro. *Exp Eye Res*. 1993;57:609-621.

52. Hynes RO. Extracellular matrix: Not just pretty fibrils. *Science*. 2009;326:1216-1219.

53. To WS, Midwood KS. Plasma and cellular fibronectin: Distinct and independent functions during tissue repair. *Fibrogenesis Tissue Repair*. 2011;4:21.

54. Elia G, Fugmann T, Neri D. From target discovery to clinical trials with armed antibody products. *J Proteomics*. 2014;107:50-55.

55. Clark RA. Potential roles of fibronectin in cutaneous wound repair. *Arch Dermatol*. 1988;124:201-206.

56. George EL, Georges-Labouesse EN, Patel-King RS, Rayburn H, Hynes RO. Defects in mesoderm, neural tube and vascular development in mouse embryos lacking fibronectin. *Development*. 1993;119:1079-1091.

57. Hynes RO. *Fibronectinsedn*. New York: Springer-Verlag; 1990.

58. van Dijk CG, Nieuweboer FE, Pei JY, et al. The complex mural cell: Pericyte function in health and disease. *Int J Cardiol*. 2015;190:75-89.

59. Wu C, Fields AJ, Kapteijn BA, McDonald JA. The role of alpha 4 beta 1 integrin in cell motility and fibronectin matrix assembly. *J Cell Sci*. 1995;108:821-829.

60. Grazioli A, Alves CS, Konstantopoulos K, Yang JT. Defective blood vessel development and pericyte/pvSMC distribution in alpha 4 integrin-deficient mouse embryos. *Dev Biol*. 2006;293:165-177.

61. Kaspar M, Zardi L, Neri D. Fibronectin as target for tumor therapy. *Int J Cancer*. 2006;118:1331-1339.

62. Villa A, Trachsel E, Kaspar M, et al. A high-affinity human monoclonal antibody specific to the alternatively spliced EDA domain of fibronectin efficiently targets tumor neo-vasculature in vivo. *Int J Cancer*. 2008;122:2405-2413.

63. Viti F, Tarli L, Giovannoni L, Zardi L, Neri D. Increased binding affinity and valence of recombinant antibody fragments lead to improved targeting of tumoral angiogenesis. *Cancer Res*. 1999;59:347-352.

64. Kalluri R. Basement membranes: Structure, assembly and role in tumour angiogenesis. *Nat Rev Cancer*. 2003;3:422-433.

65. Form DM, Pratt BM, Madri JA. Endothelial cell proliferation during angiogenesis. In vitro modulation by basement membrane components. *Lab Invest*. 1986;55:521-530.

66. Thurston G, Suri C, Smith K, et al. Leakage-resistant blood vessels in mice transgenically overexpressing angiopoietin-1. *Science*. 1999;286:2511-2514.

67. Franco M, Roswall P, Cortez E, Hanahan D, Pietras K. Pericytes promote endothelial cell survival through induction of autocrine VEGF-A signaling and Bcl-w expression. *Blood*. 2011;118:2906-2917.

68. Morikawa S, Baluk P, Kaidoh T, Haskell A, Jain RK, McDonald DM. Abnormalities in pericytes on blood vessels and endothelial sprouts in tumors. *Am J Pathol*. 2002;160:985-1000.

SUPPORTING INFORMATION

Additional Supporting Information may be found online in the supporting information tab for this article.